ENTROPY BASED IMAGE ANALYSIS FOR THE NEAR FIELD OF DIRECT INJECTION DIESEL JET

BLAISOT Jean-Bernard, YON Jérôme

CORIA-UMR 6614 : CNRS, Université et INSA de Rouen
Site universitaire du Madrillet, avenue de l'université
BP 12 76801 Saint Etienne du Rouvray, France
Phone : 33.(0)2.32.95.36.76 / fax : 33.(0)2.32.91.04.85
jean-bernard.blaisot@coria.fr jerome.yon@coria.fr

ABSTRACT

Entropy analysis is applied to backlight images of the near field of a Diesel jet produced by a single hole nozzle. The entropy is calculated through the determination of the occurrence frequency of three pixel categories associated to the dense liquid core, the dispersed liquid phase and the gas. The maps of entropy are used to determine the statistical characteristics of the spatial distribution of the three phases. The area of the region of primary atomisation is measured as a function of time and of the downstream position along the jet axis. For high injection pressure the increase of this area is supposed to be related to the mechanical vibrations occurring in the movement of the needle when the needle leaves or reaches closed or fully opened positions. Finally, spatial variation of the local maximum of the entropy is used to determine characteristic length scales of the jet interface.

1. INTRODUCTION

Reduction of pollutant emissions and improvement of Diesel combustion are being pursued with the aim of undertaking environmental issues. A better understanding of combustion processes is needed to reach this aim. The development of Diesel combustion models and the introduction of these models in CFD codes require more and more knowledge on the physics of fuel injection. Thus a more accurate description of the Diesel jet is needed in order to elaborate more realistic model for the atomisation processes and as a consequence to improve the reliability of the CFD calculations. Up to now, the calibration of numerical simulations of Diesel jets is based on measurements of the spray tip penetration, of the spray cone angle or of the far field and late drop size distribution. However, more details and information are needed concerning the characteristics of the two-phase flow emanating form the injector nozzles in the near field. Several works have been conducted by the authors on the study of the structure of the liquid jet in the vicinity of the nozzle orifice through different visualisation techniques [1][2] and through the use of a morphological analysis of two-level images [3]. Whereas visualisations of the Diesel jet presented in [1] and [2] give only qualitative results, the morphological analysis presented in [3] was a first step to the determination of quantitative parameters to describe the jet structure in the vicinity of the nozzle outlet. A new method is proposed here to study the nature of the Diesel jet in the near field. It is based on the determination of the local entropy in the image. The entropy is based on the definition of three 'states', which are the dense liquid core, the dispersed liquid phase and the gaseous phase. Entropy maps statistically quantify the Diesel jet behaviour at the nozzle outlet. A new kind of information about the spreading the jet and the dispersed phase is so obtained. The area of the region associated to primary atomisation is determined from the entropy values and compare to some results of the morphological analysis. Finally, it is showed that characteristic length scales of the jet interface can be determined from the entropy analysis.

2. EXPERIMENTAL SETUP

The experimental set-up has already been presented in previous papers [1]-[3] so only a brief description is done here. A single hole VCO type injector (diameter D_i = 200 µm, length L = 800 µm) is used. Shadowgraph images of the near field of the Diesel jet (Fig.1a) are recorded with a long distance microscope and a full frame CCD camera (763x581 pixels, 8 bits). The field of view is 0.91 mm x 1.14 mm. A very short duration light source (≈15 ns, nanolite, HSPS) is used to obtain still images of the jet. Results are reported here for injection pressure P_i = 20 and 60 MPa without back-pressure (ambient air at atmospheric pressure and temperature). An infrared-led transceiver is placed at the nozzle exit in order to detect the start of injection (SOI). SOI correspond thus to the time when the fuel flowing out from the injector stops the light. Images are recorded for different times T_{aSOI} after SOI. These times as well as the

curve of the lift of the needle are shown in Fig.1b. The needle lift curve for P_i = 60 MPa presents a stationary portion for T_{aSOI} = 725 to 1205 µs and two transient parts at the beginning and the end of injection.

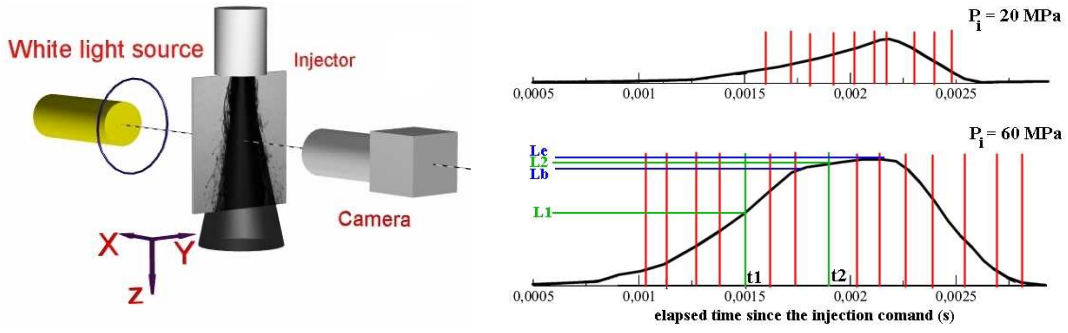

(a) (b)

Figure 1 : Arrangement of the injector and the visualisation system in a backlight configuration (a). Needle lift curves and illumination times (b) for P_i = 20 and 60 MPa.

3. PRINCIPLE OF THE ENTROPY BASED ANALYSIS

Grey level images (see Fig.2a) are converted in two-level images through a two-stage image thresholding technique combining one binary image, based on a classical grey level threshold, and another one binary image, based on a wavelet transform process. The grey level threshold is defined as the mean level between the darkest grey level and the most populated bright level obtained from the global grey level histogram of each shadowgraph image. The first binary image is obtained by application of this threshold. Unfocused droplets or ligaments are missed in this binary image. A second binary image is obtained by application of a threshold on the result of a wavelet transform (WT) applied to the image. This WT is used to detect concavity and convexity in the grey level image using a *Mexican-Hat* as the mother function [4]. The grey level image is considered here as a 3D surface where the grey level is the height of the surface normally to the image plane. This surface is convex at the outline of the image of a liquid object, even if this object has a small contrast that prevents it from being detected by the first thresholding technique. The binary image obtained from the thresholding of the WT contains thus the convex portions of the image. The combination of the two binary images is a complete representation of the continuous and dispersed phases of the Diesel jet (Fig.2b).

Each pixel of the two-level image is associated to one of the three possible states identified in the images that are: (1) the dense liquid core at the centre of the jet, (2) the dispersed liquid phase which is constituted of liquid portion not attached to the dense core and (3) the gaseous phase. It was shown in a previous study that the dense liquid core was not always so dense as it could include gas cavities of tubular shape [2]. However, the interface of the liquid core is so corrugated that it is very difficult to determine its real structure and its real location through backlight visualisations. This is why our definition for the dense liquid core is in fact relative to the optical density that prevents separation of ligaments or droplets from the real dense core in this region.

The frequency at which each state occurs is measured from a series of N = 400 images, for each pixel of the image. For a given pixel, this frequency represents the probability p_S to be associated to one of the three states S = 1, 2 or 3. The normalized entropy E of this pixel is thus given by:

$$E = -\frac{p_1 \ln p_1 + p_2 \ln p_2 + p_3 \ln p_3}{\ln 3} \qquad (1)$$

The normalized entropy E is 0 when only one state is 'seen' by the pixel and is 1 when the three probabilities are identical. An example of entropy mapping is shown in Fig.2c. The pixels of the centre of the jet which are always in state 1 and those at the border of the image which are always in state 3 have an entropy E = 0. Conversely, the pixels at the outline of the jet which can be either in one of the three states have a non zero entropy.

(a) (b) (c)

Figure 2: Image of the Diesel jet (a). Two-level image of the jet (b) where the continuous (grey) and the dispersed (black) phases are identified. Mapping of entropy (c) associated the jet image in (a). Pi = 20 MPa and T_{aSOI} = 205 µs.

A particular case to be considered corresponds to a pixel covered by at most two of the three possible states. The maximum entropy for this pixel is obtained for the condition of identical probabilities between the two covered states. For example, taking $p_1 = p_2 = 0.5$ and $p_3 = 0$ leads to $E = E_2 = \ln 2/\ln 3 \approx 0.631$. So a pixel seeing only two states has an entropy in the range $]0;E_2]$. As soon as the third state is covered, the corresponding entropy is greater than E_2. Pixels for which $E > E_2$ are so concerned with the three states, i.e. the continuous liquid phase, the dispersed liquid phase and the gaseous phase are encountered at this location. These pixels are thus located at the outline of the jet core in a region of transition between dense and dispersed liquid phases, referred here as the primary atomisation zone.

It must be noted here that the entropy has to be considered when more than two 'states' can be associated to the pixels of the images. On the contrary, the classical mean and standard deviation values for two-level images give the same kind of information, although entropy values are not dependent on the grey level associated to each state.

Moreover, it is possible to define a global mean value $\overline{E}$ of the entropy for the images. This number thus depends on the number N of images taken into account for the calculation of $\overline{E}$. The curve of the global entropy $\overline{E}$ versus N tends to a limit value when the series is statistically representative of the phenomenon. If an artefact occurs during the recording of the image series (no jet, no light source or electronic interferences), this is expressed by a discontinuity of the mean entropy of the sub-series and the corresponding image is then easily eliminated from the series.

The entropy mapping of the Diesel jet is presented in the next section. In the section after, the analysis of the primary atomisation zone is proposed.

4. ENTROPY MAPS OF THE DIESEL JET IMAGES

Entropy maps of the jet for $P_i = 20$ and 60 MPa are presented in Fig. 3 for 10 and 15 times after SOI respectively. The jet flow is from the left to the right on the figure and the two sides of the jet are treated separately. The maps for $P_i = 20$ MPa (Fig. 3a) indicate that the region of transition between the dense core and the surrounding air increases downstream for the two sides of the jet. There is a steep increase of the entropy from the dense core to the dispersed phase region indicating that the edge of the dense core is very reproducible. It must be noted here that entropy maps are computed from series of 400 images so the dense core edge location is the same over 400 injections.

Apart for the first and last times after SOI, the entropy maps does not deeply change along the injection time. However, the width of the region of high entropy slightly increases with the needle lift. The right side of the jet seems also to spread out a little bit more than the left side, especially for $T_{aSOI} = 305$, 405, and 505 µs in Fig.3a.

The jet presents an evident asymmetry for $P_i = 60$ MPa (Fig.3b). For the left hand side of the jet, the region of non-zero entropy is thinner during the stationary part than during the transient parts of the injection, indicating that there is a sharp transition between dense and dispersed phases at these times and also that no cycle-to-cycle fluctuation occurred. The shape of the left hand side of the jet is thus very stable and reproducible during the stationary period. The location of the inner limit of the non-zero entropy region is roughly the same over the stationary period but this limit changes in position during the transient periods. This is due to the fact that during the transient periods, the jet is being formed or disappears and so the dense liquid phase is not always present along the axis of the jet. This is particularly true at the end of the injection ($T_{aSOI} = 1565$ and 1685 µs).

The right hand side of the jet is quite similar to the left hand side during the transient periods but presents strong differences during the quasi-stationary part of the injection. Indeed, for this period, the entropy maps show a hook shape with a small second branch, oriented at a higher deviation angle from the jet axis than the main branch located along the dense liquid phase. This small branch results from a phenomenon of ligament striping occurring at a particular location of the nozzle edge, only during the stationary part of the injection and for injection pressures higher than 25 MPa. This phenomenon was already mentioned in the previous analyses realised with this nozzle [1]-[3]. The image in Fig. 4a shows this phenomenon. A ligament is linked to the nozzle outlet at the upper side of the image, so this ligament is associated to the same state than the dense part of the jet. The three states are thus encountered in this region and so the entropy reaches value higher than E_2. The region downstream the hook shape on the entropy mapping is constituted of gas and liquid dispersed phases only as indicated by the value of entropy lower than E_2.

However, the hook shape is replaced by a single broad zone of high entropy for the particular time $T_{aSOI} = 845$ µs. The shape of the right part of the Diesel jet changes at this time as can be seen in Fig. 4b. The morphological analysis showed that for this particular time delay, the mean ligament length presents a maximum in this region [3]. Indeed, a high number of ligaments are formed at this time and these ligaments are connected to the dense core by the image processing sequence. In fact, the liquid density is too high for the ligaments to be separated. As a consequence, the state $S = 1$ is count in this region even it is far from the dense core and the entropy can reach value higher than E_2. A little bit time later, for $T_{aSOI} = 965$ µs, the jet is again in the same state than before $T_{aSOI} = 845$ µs as can be seen in Fig.4c.

5. PRIMARY ATOMISATION ZONE

The primary atomisation zone is defined as the region in the entropy map for which $E \geq E_2$, i.e. where the three states are counted during a series. The area A_a of this zone indicates the spreading of the transition zone between the liquid core and the dispersed phase. This area is determined for each downstream position Z: the number of pixels satisfying $E \geq E_2$ along a line perpendicular to the jet axis is taken as the local downstream atomisation zone area. Results are presented in Fig. 5 for the variation of A_a versus T_{aSOI} for $P_i = 20$ and 60 MPa. As mentioned for the analysis of the entropy maps, the behaviour for $Pi = 20$ and 60 MPa are different. Indeed, for $P_i = 20$ MPa (Fig. 5(a))

the atomisation area presents a gradual variation in space and in time whereas steep changes are observed for P_i = 60 MPa (Fig. 5(b)). For P_i = 20 MPa, the atomisation area increases along the downstream position. The maximum is reached just before and after the maximum of the needle lift for $T_{aSOI} \approx 600$ µs. It must be noted here that for this injection pressure, the maximum lift position reached by the needle is far lower than the fully opened position.

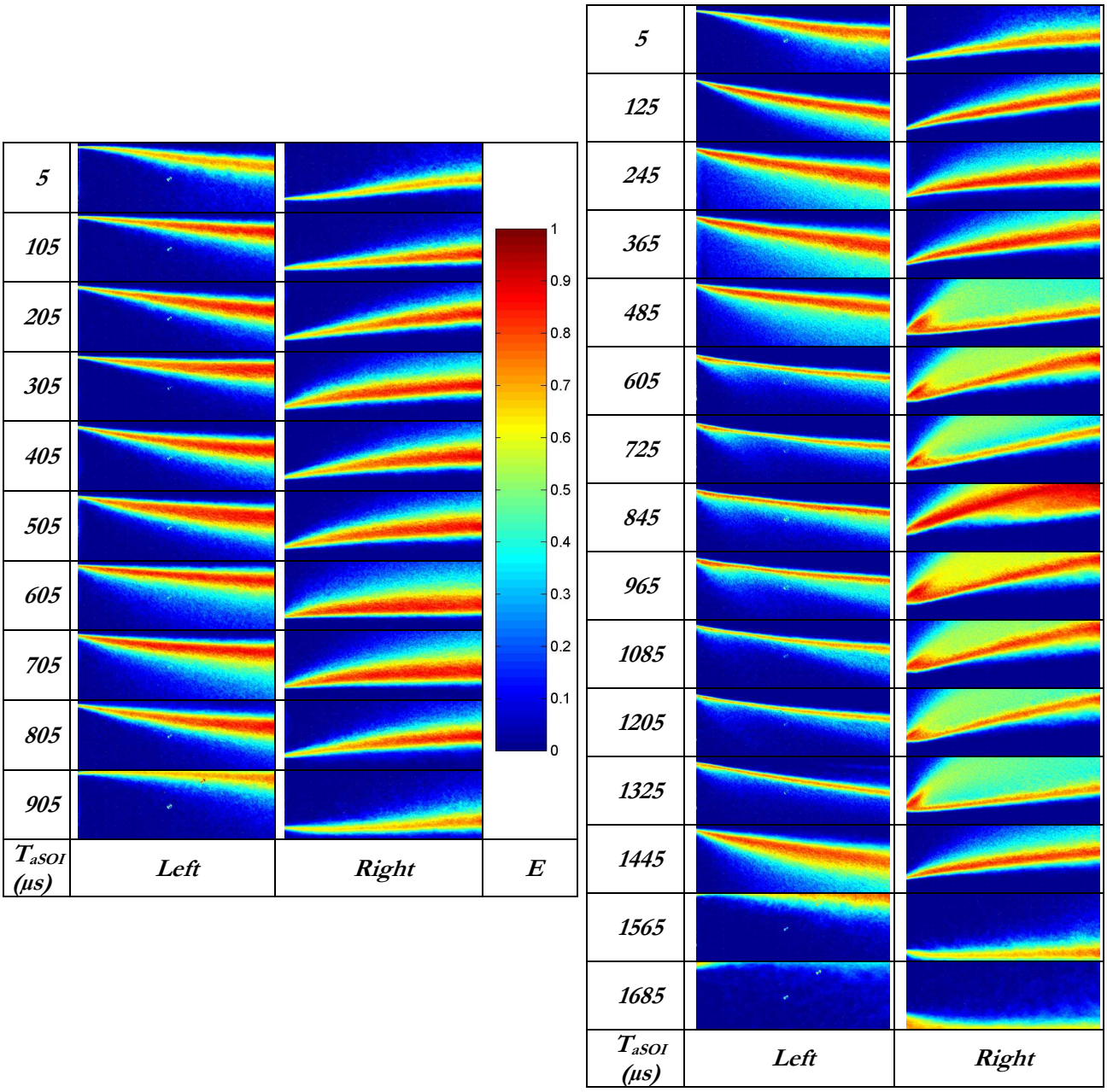

(a) (b)

Figure 3: Entropy maps of the Diesel jet for P_i = 20 MPa (a) and 60 MPa (b).

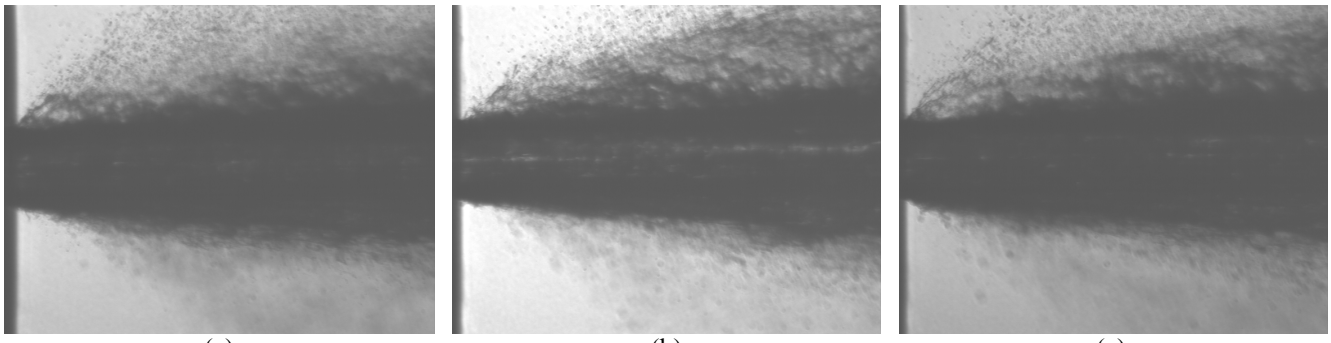

(a) (b) (c)

Figure 4: Image of the Diesel jet during the stationary period of the injection for Pi = 60 MPa. (a) T_{aSOI} = 725 µs, (b) T_{aSOI} = 845 µs, (c) T_{aSOI} = 965 µs.

For P_i = 60 MPa there are three periods of high atomisation area, at the beginning, at the end and during the quasi-stationary part of the needle lift. As mentioned above, a ligament is connected to the nozzle exit during the period between T_{aSOI} = 485 and 1325 µs. This creates a region of middle level of atomisation area around Z = 0.1 mm but A_a decreases right downstream this region to very low levels, except for $T_{aSOI} \approx$ 845 µs.

The atomisation area is high when the needle is nearly closed or fully opened and decreases during the transient periods of the needle movement, i.e. between minimum and maximum lift positions. It was concluded from these results and other experiments not presented here that for injection pressure leading to a complete lift of the needle, the atomisation area presents steep changes in time. In these cases, periods of high atomisation area correspond to the beginning or the end of the needle movement. Measurements of the mechanical vibrations of the injector showed that high frequency oscillations occur when the needle leaves or reaches a stable position (closed or fully opened). The morphological analysis of the jet also showed that for these moments, the jet cone angle seems to oscillate in time. Whereas no clear relation was found between mechanical and hydrodynamic oscillations, it is supposed that the mechanical movement of the needle when it leaves or reaches a stable position induces hydrodynamic changes responsible of the appearance of the high atomisation area. During the transient movement of the needle, the atomisation area keeps rather at low levels.

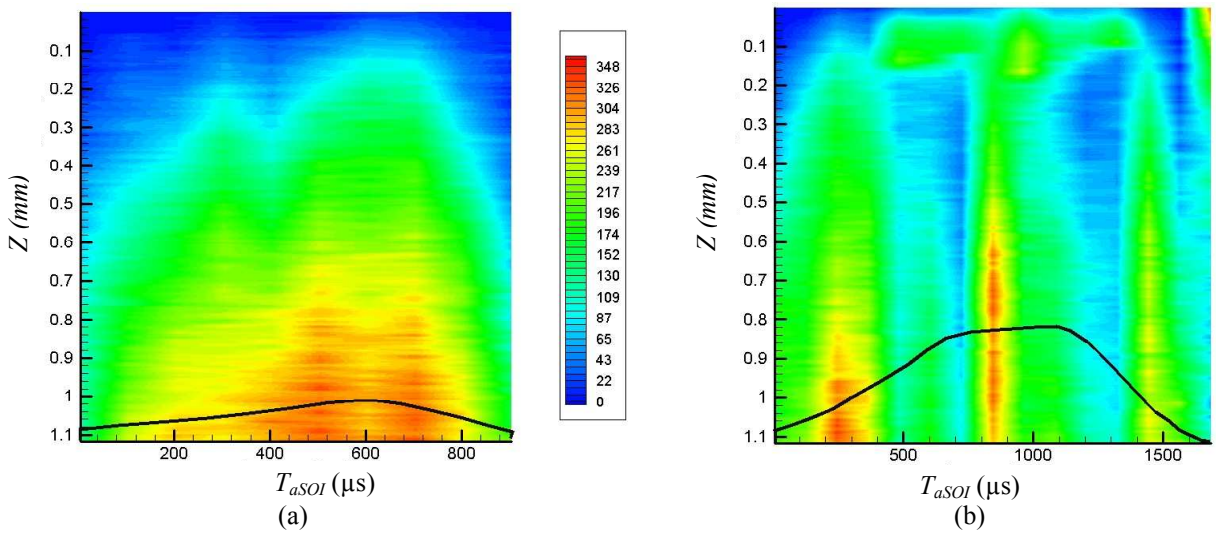

Figure 5: Primary atomisation zone area A_a along the jet axis as a function of time after SOI: (a) P_i = 20 MPa, (b) P_i = 60 MPa. Entropy levels correspond to the number of pixels on a line for Z = cste satisfying $E \geq E_2$. The needle lift curves are indicated at the bottom of the figures as plain black lines.

The entropy analysis can also brings out information about the spatial periodicity that can be found in the images along the jet interface. A test was carried on a series constituted of synthetic images presenting a periodic pattern randomly placed relatively to the image border. The characteristic length scale of the pattern is retrieved in the spatial variation of the entropy along the direction where oscillations occur, whatever the number and the arrangement of the images in the series. So, as soon as a given periodicity exists in the images, the entropy analysis can put emphasis on the characteristic scale of this periodicity.

This particular advantage of the entropy analysis was tested to determine a length scale characteristic of the atomisation process in the near field of the nozzle outlet. Indeed, such a length scale exists, induced by the destabilisation process caused by the high velocity difference at the jet interface and it should be present also in the spatial distribution of ligament and droplets in the primary atomisation zone.

To determine such a length scale, the spatial variation of the entropy must be analysed. A small region on one side of the entropy map is first considered as indicated by the lighter rectangular zone in Fig.6a. This region is connected to the nozzle outlet and covers approximately 0.2 mm along the vertical direction. For each downstream position Z, the maximum entropy is taken and reported in a graph as shown in Fig.6b. The maximum entropy is always greater than E_2 and globally increases along the vertical axis. This increases is due to the fact that the farthest from the injector, the more spread out the dispersed phase and so the more equi-probable the three states.

A spatial fluctuation is also obvious on this figure. The variation of 10 % of the magnitude of the local entropy is sufficiently significant to be considered as characteristic of local differences in the spatial distribution of the three states. A mean period of the order of 20 µm appears to the naked eyes for P_i = 60 MPa and T_{aSOI} = 245 µs when considering the local peaks of the entropy between Z = 0.04 and 0.14 mm. This length scale is in accordance with length scales determined from destabilisation models [5]. However, such a length scale was not always clearly identifiable and so no parametric study was conducted. Nevertheless, we think that more developments need to be fulfilled in order to bring out quantitative measurement from the entropy analysis. This could be an alternative way to calibrate CFD codes in the future.

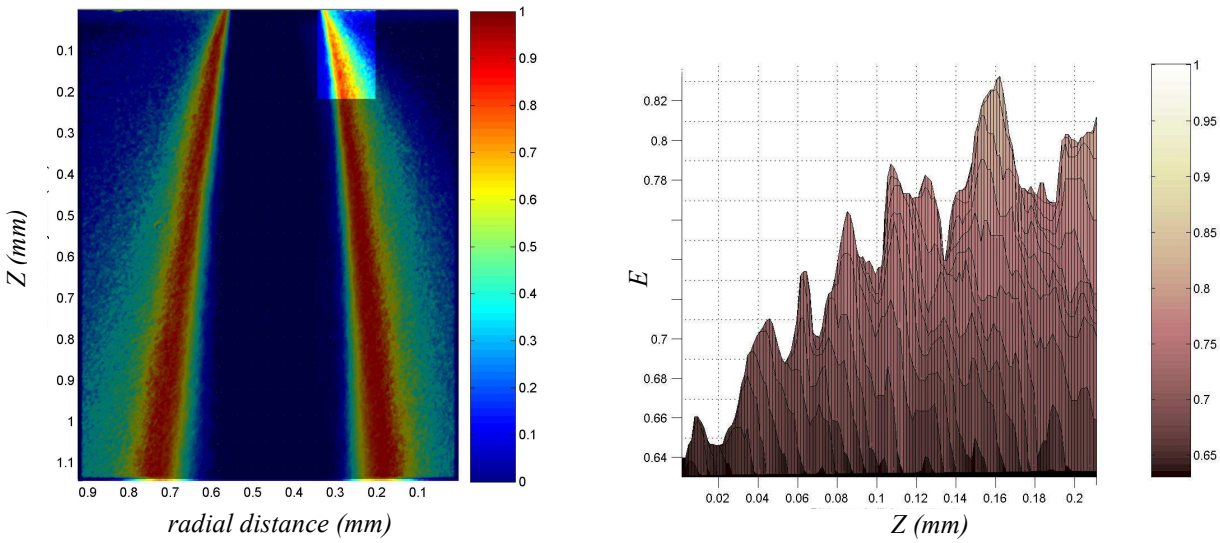

(a) (b)

Figure 6: Spatial oscillations of entropy determined along the maximum entropy crest P_i = 60 MPa and T_{aSOI} = 245 µs. (a) region of interest. (b) Variation of the entropy long the crest.

6. CONCLUSION

Through the first results presented here it seems that this analysis is a promising tool for the statistical characterisation of the Diesel jet. The maps of entropy are used to determine the spatial distribution of the three phases considered. The steep transition between the dense liquid core and the dispersed phase indicated the absence of cycle-to-cycle fluctuations. The area of the region of primary atomisation showed two different behaviours for the two injection pressures used in the experiments. For the lower injection pressure, a gradual variation of the area of the primary atomisation zone is found whereas for the higher injection pressure this area presents steep variations versus time. The increase of this area is supposed to be related to the mechanical vibration occurring in the movement of the needle when the needle leaves or reaches closed or fully opened positions. The determination of a characteristic length scale on the jet interface from the analysis of the spatial variation of the local maximum of the entropy could be useful for the validation of CFD codes. However, further developments need to be achieved in order to determine the most significant length scale of the interface for all injection conditions. The objective is now to apply this analysis to multi-hole nozzles in realistic ambient conditions.

NOMENCLATURE

A_a: Area of the primary atomisation zone
D_i: Nozzle diameter
E : Normalized entropy
E_2: Maximum normalized entropy for only 2 states over 3
L: Nozzle length
p_s: probability of state S
P_i : Injection pressure
S: States associated to the pixels
T_{aSOI}: Time after start of injection
X,Y,Z: Spatial coordinates

REFERENCES

[1] J. Yon, J.B. Blaisot and M. Ledoux, External and internal behaviour of the near field Diesel jet at high injection pressure: dual source visualization and multiple angles tomographic experiments, 18th ILASS-Europe, Zaragoza, Spain, 2002.

[2] J. Yon, J.B. Blaisot and M. Ledoux, Unusual laser-sheet tomography coupled with backlight imaging configurations to study the Diesel jet structure at the nozzle outlet for high injection pressures, J. Flow Visualization and Image Processing, Vol. 9, pp. 53-73, 2002.

[3] J. Yon and J.B. Blaisot, Morphological analysis of the Diesel jet at the nozzle outlet, ICLASS, Sorrento, Italy, 2003.

[4] J. Yon, Jet Diesel Haute Pression en Champ proche et lointain : Etude par imagerie, Ph.D dissertation of the university of Rouen, France, 2003.

[5] S.P. Lin and Z.W. Lian, Mechanisms of the breakup of liquid jets, AIAA Journal, Vol. 28, 1, pp. 120-125, 1988.